Talanta 284 (2025) 127215

Contents lists available at ScienceDirect

Talanta

journal homepage: www.elsevier.com/locate/talanta

Gold leaf electrodes for UV/Vis spectroelectrochemical determination of ortho-diphenols in extra virgin olive oil

Michele Abate, Gino Bontempelli, Nicolò Dossi *

Sustainable Analytical Instrumentation Laboratory, Department of Agrifood, Environmental and Animal Science, University of Udine, via Cotonificio 108, I-33100, Udine, Italy

ARTICLE INFO

Keywords:
Gold leaf electrodes
Spectroelectrochemistry
Portable analytical devices
Ortho-diphenols
Extra virgin olive oil

ABSTRACT

A simple and easily replicable technique is here presented for assembling planar electrochemical cells based on gold-leaf electrodes using ordinary tools and a do-it-yourself approach. These devices have been profitably used to perform spectroelectrochemical measurements in the reflectance mode demonstrating for the first time how the use of gold-leaf electrodes can offer a viable and low cost alternative to traditionally used electrochemical platforms assembled by gold vapor deposition or screen printing.

After optimization of fabrication parameters, the electrochemical and spectroelectrochemical characterization of these cells was performed by using potassium hexacyanoferrate(II) as redox probe.

Then, hydroxytyrosol has been selected as model to develop an innovative and so far never presented spectroelectrochemical method for the determination and quantification of ortho-diphenol antioxidants in extra virgin olive oil. The results achieved allowed us to preliminary evaluate the electrochemical oxidation mechanism of hydroxytyrosol at gold leaf electrodes and then to select the best wavelength for its spectroelectrochemical determination.

The approach developed enabled to evaluate hydroxytyrosol concentrations from both the electrochemical and spectroscopic signals with repeatable and comparable results. Comparison between electrochemical and optical determinations performed on real sample demonstrates that the two methods can be used indistinctively, proving that spectroelectrochemistry represents an autovalidated technique able to provide reliable results thanks to complementary information that are simultaneously obtained from electrochemistry and spectroscopy.

1. Introduction

In recent years, the growing attention toward environmental, social, and economic sustainability has driven the development and diffusion of Green Analytical Chemistry (GAC) and Democratic Analytical Chemistry (DAC). These emerging fields focus on developing affordable, user-friendly, and environmental friendly analytical tools that are accessible to a wide audience of users, even those lacking specialized training. GAC and DAC principles emphasize the use of readily available materials, minimization of solvent and energy consumption, ensuring at the same time operator safety for the development of innovative analytical methods and devices [1–3]. From this perspective, electrochemistry aligns well with GAC and DAC principles due to its ability to perform direct measurements with minimal sample preparation, often requiring low energy and solvent consumption [4,5]. Moreover, electrochemical instrumentation can be easily miniaturized and made portable for field analysis, by using low cost components and simple fabrication techniques [6].

Several studies have explored the use of alternative materials in order to follow a sustainable approach also in the manufacturing phase of electrochemical cells. In this context, paper and bioplastics, also from recycled wastes, have been successfully employed as electrode supports for planar configurations, which are best suited for the use of small sample volumes to be analyzed [7–9]. Graphite and carbon-based materials are in general the most widely used conductive materials due to their easy availability and low cost [10–12]. Although these aspects are particularly relevant in the choice of electrode material, specific analytical requirements necessitate the use of noble metals such as gold and platinum. For example, gold, with its high electrical conductivity, electrocatalytic properties, biocompatibility, and ability to reversibly bond with thiols for surface functionalization, remains a desirable material in electrochemistry, in particular for electrocatalysis and

* Corresponding author.
E-mail address: nicolo.dossi@uniud.it (N. Dossi).

https://doi.org/10.1016/j.talanta.2024.127215
Received 30 July 2024; Received in revised form 31 October 2024; Accepted 12 November 2024
Available online 22 November 2024

biosensing [13]. Traditional gold electrode production methods, such as Chemical Vapor Deposition (CVD) and Physical Vapor Deposition (PVD), involve the deposition of a thin gold layer on a surface, often combining lithographic or photolithographic techniques. These methods require expensive equipments and clean rooms, limiting their accessibility and sustainability [14]. Gold Screen-Printed Electrodes (Gold SPEs) offer an alternative approach, utilizing gold-based inks applied through a mask. This method simplifies production and eliminates the need for clean rooms [15,16]. Alternatively, inkjet printing can be used to deposit gold-based inks directly onto various materials like paper, Kapton, and plastics, as polyethylene terephthalate (PET) [17–19]. Both SPEs and inkjet-printed gold electrodes can incorporate additional materials in their inks, which may influence their analytical performance. However, the formulation of the ink and the type of substrate in which the conductive material is deposited can lead to great variability in the electrode response, just as contact with solvents can alter their properties [20]. Moreover, these electrodes are typically disposable to prevent carry-over and surface fouling, becoming non-recyclable waste. Gold leaf, a thin sheet of pure gold that is hammered into a very thin foil commonly used for art and food decorative purposes, presents a very promising alternative for electrode fabrication at very low cost. In fact, it offers higher purity than inks and can be processed using simple and inexpensive techniques. Gold Leaf Electrodes (GLEs) can be produced at very low cost, without requiring special equipment, and provide a good electrode surface, aligning well with GAC and DAC principles [21–23].

The efficiency of gold leaf has already been demonstrated in various electrochemistry applications [24,25], including the determination of L-tyrosine [26] or, in biosensing applications, for the detection of DNase [13].

When relying only on electrochemistry, there is no need to stress that the presence of interfering substances or matrix effects can hinder the identification of specific molecules, leading to false positives/negatives. Hyphenating electrochemistry with other techniques, such as spectroscopy, allows the exploitation of different chemical properties of the analyte, providing complementary and independent information [27]. This approach can be used to overcome the limitations of single-technique analysis such as passivation problems of the electrode surface, excessive sample turbidity or limited quantification range, enhancing selectivity and sensitivity. Several studies performed measurements and determinations using dual-mode devices, in which spectroscopic and electrochemical measurements were used together, but they were conducted not simultaneously, exploiting simultaneous availability of data for the construction of two different calibration plots relative to two independent signals to be used for mutual control [28–30]. Instead, spectroelectrochemistry (SEC) is a hybrid analytical technique that simultaneously provides electrochemical and spectroscopic information on molecules involved in redox reactions [31,32]. It was continuously improved combining electrochemical techniques with an ever-increasing number of spectroscopic methods (UV/Vis, IR, Raman, NMR). As a result, it has emerged as a valuable tool for characterizing molecules, studying reaction mechanisms and their kinetics, but it is still underutilized for quantifying substances in complex matrices and improving detection ranges during analysis [33].

Different cell configurations have been proposed for UV/Vis-SEC, aimed at optimizing transmittance or reflectance measurements. For transmittance measurements, the use as electrodes of either thin conductive layers deposited directly on quartz, plastic, or glass-based substrates, or mesh electrodes inserted into the optical measurement cell was recommended [34–37]. For reflectance measurements the use of polished and optically reflecting metals, typically platinum or gold, was instead suggested [38,39].

Recently, SPE electrodes with SEC were successfully employed for the SEC determination of various molecules, including folic acid and dopamine [40–43]. In particular, in the case of dopamine, the oxidation of its catechol group results in the loss of two electrons and two protons, leading to the formation of *o*-quinone which displays a characteristic absorption band at 390 nm, unlike catechol [44]. It is important to note that an *o*-diphenolic structure of this type is found in many compounds present in foods that exhibit high antioxidant power. For instance, olive fruits contain catechol derivatives such as oleuropein (Oleu), the main bioactive compound present in olives, and hydroxytyrosol which is the main breakdown product of oleuropein in olive oil [45,46].

The determination of hydroxytyrosol in food is crucial because it is a strong antioxidant used as a marker for the quality and health benefits of olive oils, a common condiment fat in the Mediterranean diet. Several studies have shown that its high antioxidant activity leads to significant health benefits, including the reduction of the oxidative stress, the modulation of the immune response and of the exposure to antibacterial and antiviral properties [47–49].

In this study, an innovative, low cost, and easy-to-fabricate approach for assembling electrodes arranged in a planar configuration using gold leafs as the conductor material to perform spectroelectrochemical measurements is presented for the first time. Gold Leaf Electrodes (GLEs) were produced using readily available and recyclable materials and were cut with a common cutting plotter, according to GAC and DAC principles.

After a preliminary evaluation of their performance by hexacyanoferrate(II) as the prototype analyte, the capabilities of UV/Vis-SEC conducted at GLEs were evaluated in the study of both the oxidation mechanism of hydroxytyrosol and its quantitative determination in olive oil samples.

2. Materials and methods

2.1. Chemicals

Potassium hexacyanoferrate(II), hydroxytyrosol [2-(3,4-dihydroxyphenyl)-ethanol] (HTy), tyrosol [2-(4-hydroxyphenyl)-ethanol] (Ty), potassium nitrate, sulphuric acid, methanol, ethanol, ethyl acetate and pentane were purchased from Sigma-Aldrich (Sigma-Aldrich, Milan, IT). They were of analytical reagent grade and were employed without further purification.

Aqueous 0.1 M potassium nitrate and 20 mM sulphuric acid solutions were prepared in ultrapure water obtained from an Elgastat UHQ-PS system (Elga, High Wycombe, UK) and used as supporting electrolytes in voltammetric and spectroelectrochemical experiments.

Potassium hexacyanoferrate(II) stock standard solution (10 mM) was prepared by adding weighed amounts to known volumes of the 0.1 M KNO_3 solution. Hydroxytyrosol and tyrosol stock standard solutions (10 mM) were prepared by adding weighed amounts to known volumes of 20 mM sulphuric acid. When needed, controlled amounts of these stock solutions were diluted to the desired concentrations with the same solution prior to each experiment. A HTy solution (20 mM) was prepared in ethyl acetate to prepare fortified oil samples.

Spectroelectrochemical and voltammetric measurements were carried out using an UV/Vis SPELEC 200–900 nm instrument (Metrohm-DropSens, Varese, IT) controlled by a DropView SPELEC software.

Voltammetric measurements were carried out in a conventional cell using a gold working electrode (CH Instruments, Texas, USA), a platinum counter electrode and an Ag/AgCl, 3 M KCl reference electrode (CH Instruments, Texas, USA).

Gold Leaf Electrodes (GLEs) were assembled using 24-carat gold leaves (AP Verona, Verona, IT), silver-based ink pen (CircuitScribe, USA), double-sided 200 μm thick adhesive tape (300 LSE, 3 M, St. Paul, MN, USA), self-adhesive vinyl foils (Metamark 4 Series, Metamark Sign Vinyl, Woking, GB) and polypropylene (PP) recovered from cosmetic packaging.

2.2. Fabrication of GLEs

A series of four identical three electrode GLE cells, whose design was similar to that adopted for commercial screen-printed electrodes and

consisting of a working (area 12.6 mm^2), a pseudo-reference and a counter electrode was firstly drawn by a Silhouette studio software version 4.3 (Silhouette CAMEO®, Micronet Italia, Milano, IT).

The layout design was cut into vinyl adhesive sheet with the cutting device and the unwanted parts were peeled off with tweezers (Fig. 1a and b). Then, the stencil with the three electrodes layouts was applied to a double-sided adhesive tape previously peeled on one side (Fig. 1 c). Gold leaf was placed on the exposed adhesive area and gently pressed with a cotton stick to ensure good adhesion (Fig. 1d and e). Excess gold leaf was removed with a spatula and then patterned platforms were cut into pieces to obtain single GLEs (see Fig. 1 f). Finally, to complete the fabrication of GLEs, a polypropylene (PP) support was applied to the other side of the double-sided adhesive tape and a conductive ink was applied with a silver-based ink pen in the area provided for contacts to give a satisfactory rigidity to the platform and to ensure good electrical connections (Fig. 1 g). Thin strips (9 mm in length, 9 mm in width) were placed onto the top of the GLEs to delimitate the active working surface and to protect electrical connections from the contact with liquid samples (see Fig. 1 h). Before the first use, GLEs were washed using an ethanol-water solution (50/50 % v/v) to remove any residual dirt from their handling.

2.3. Voltammetric and UV/Vis spectroelectrochemical measurements at GLEs

Preliminary voltammetric measurements were conducted by applying a small volume of sample (50 μL) directly onto the GLE which was placed in the horizontal position on a planar surface (drop mode). The electrochemical behavior of electrodes was studied using a 0.1 M KNO_3 solution containing 1 mM of $K_4[Fe(CN)_6]$. This analyte was chosen as the redox prototype in view of its well-known reversible electrochemical behavior. Cyclic voltammetric experiments were run in the potential window from −0.20 V to +0.70 V *vs.* an Ag/AgCl, 3 M KCl reference electrode or from −0.30 V to +0.60 V *vs* the gold pseudo-reference electrodes.

UV/Vis-SEC experiments were carried out using the SEC cell for reflectance experiments (DRP-REFLECELL, Metrohm-DropSens) and a reflection probe (DRP-RPROBE, Metrohm-DropSens), by performing a small modification consisting in the replacement of the o-ring present in the original configuration with a circular rubber gasket made using the cutting plotter. This modification was made to limit the crushing of GLEs and avoid damaging the conductive tracks.

To perform UV/Vis-SEC experiments, the GLE was placed in the lower body. Then, the upper body was attached to the lower part, exploiting the four magnets present in both pieces. Finally, 50 μL of the test solution was added, making sure that this drop covered completely the three GLE electrodes and the optical probe was introduced in the dedicated hole at the top for reflectance measurements.

To validate the functioning of GLEs, UV/Vis-SEC tests were firstly performed using a 0.1 M KNO_3 solution to which 10 mM of $K_4[Fe(CN)_6]$ were added. Experiments using HTy were then carried out using the 20 mM sulphuric acid solution as electrolyte and varying the HTy concentration from 10 to 10000 μM for the construction of the calibration curve.

During SEC experiments in the presence of the sole HTy, the potential was scanned in the range from −0.30 V to +0.60 V, starting from −0.10 V, for $K_4[Fe(CN)_6]$ and from −0.40 V to +0.50 V, starting from 0 V, by using different scan rates and starting all the experiments in the anodic direction. This range was extended to +0.70 V when also Ty was introduced. The evolution of absorption spectra was collected from 200 to 900 nm during cyclic voltammetric experiments. In all UV/Vis-SEC experiments, the first spectrum of the sample (−0.10 V and 0 V for $K_4[Fe(CN)_6]$ and HTy, respectively) was taken as reference, and the absorbance change was recorded and expressed as ΔAbs with respect to the reference spectrum during the potential scan. Time-resolved UV/Vis-SEC measurements were performed using an integration time of 15 ms.

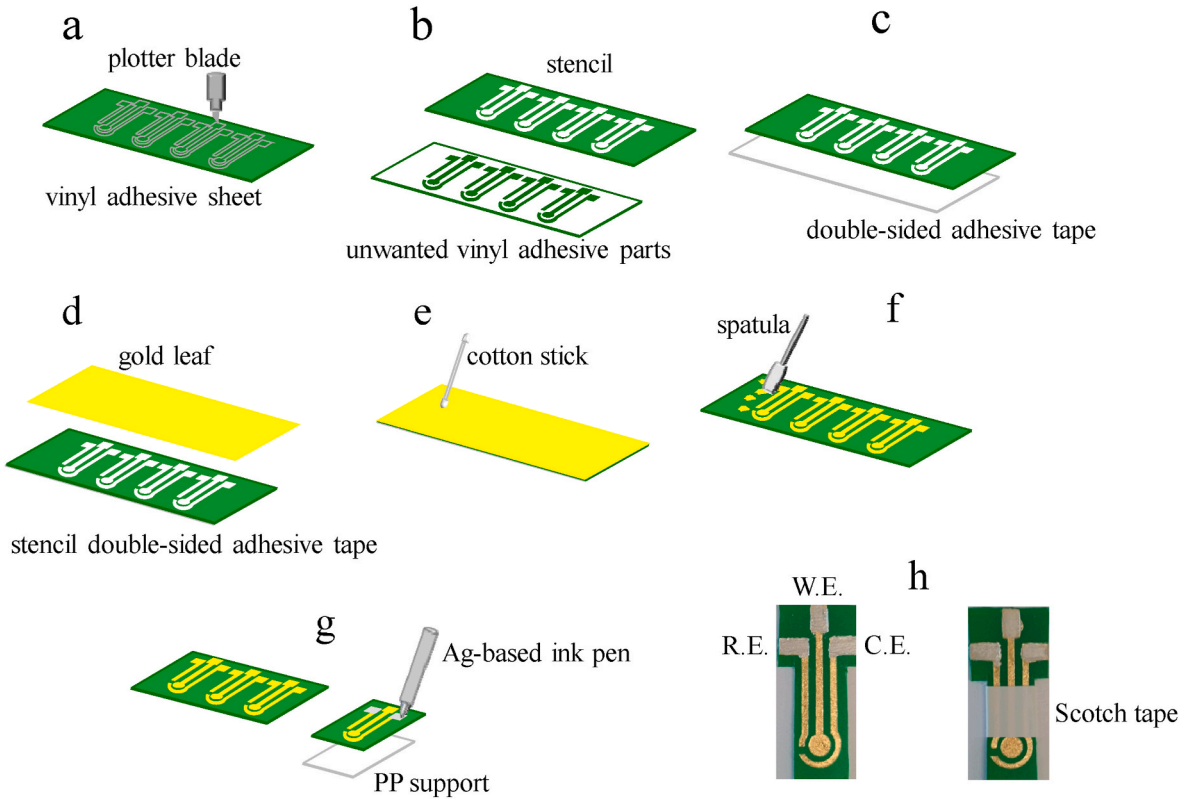

Fig. 1. Schemes of the assembly procedure of the GLEs (a–g) and picture of the assembled devices (h). W.E., R.E. and C.E. are the working, pseudo-reference and counter electrodes, respectively.

As to the construction of the calibration plot for HTy, the maximum absorbance recorded during the potential scan for the concentrations considered, that was acquired at the potential of +0.20 V in the reverse direction, was used to calculate the ΔAbs with respect to the blank solution.

2.4. Real sample preparation

Two high quality extra virgin olive oils (EVOOs), containing blends of different varieties and with high percentage from cultivar *Coratina*, and one sunflower oil were purchased in a local market. They were analyzed with a slightly modified established extraction procedure [50,51], according to the IOC protocol [52], involving no acid hydrolysis of the extracted phenolic compounds. Hydroxytyrosol and other hydrophilic phenols were extracted by Vortex mixing (1 min) 2 g of oil sample with 2 mL of a methanol-water solution (80/20 % v/v). Then, the mixture was centrifuged (5000 rpm for 25 min) and the surnatant was transferred into a 10 mL flask. The polar phase was washed with 2 mL of pentane to eliminate oil residues and, after the pentane removal, the solution was concentrated to 300 μL by nitrogen flowing. It was finally reconstituted with 300 μL of 20 mM H_2SO_4 aqueous solution before analysis. Fortified EVOO and sunflower samples were prepared adding HTy by using the ethyl acetate standard solution.

3. Results and discussion

3.1. Electrochemical characterization of GLEs

Preliminary voltammetric investigations were performed to test the assembled GLEs. When cyclic voltammograms were recorded with the sole supporting electrolyte (0.1 M KNO_3), neither voltammetric interfering peaks were detected nor any significant electrical noise was observed, thus supporting the good quality of the gold used and the validity of the construction method.

Further insight on this topic was gained when a 1 mM solution of hexacyanoferrate(II) in 0.1 M KNO_3 was analyzed. As shown in Fig. 2 (red line), cyclic voltammetric profiles recorded at scan rate of 50 mVs^{-1} using an external Ag/AgCl (3 M KCl) reference electrode displayed a satisfactorily reversible anodic-cathodic system superimposed to a rather flat baseline with a distance of the backward peak from the forward one (E_{pa}–E_{pc}) of about 70 mV.

As shown in this Figure (black line), comparable results were obtained using a gold disk electrode immersed in a conventional electrochemical cell containing the same reference solution of hexacyanoferrate(II). Despite the different peak heights, due to the different sizes of the electrode areas, voltammetric profiles showed peaks with very similar anodic and cathodic potentials at +0.24 and + 0.17 V, respectively.

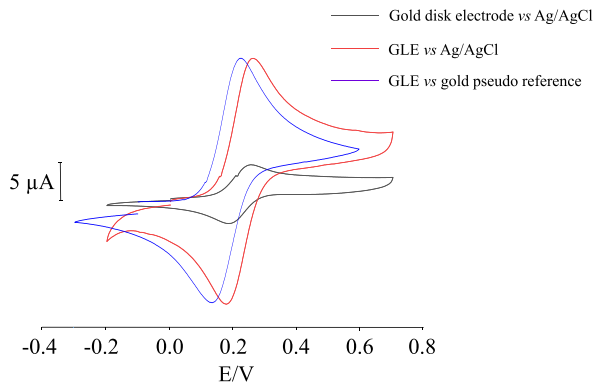

Fig. 2. Cyclic voltammetric profiles recorded at a gold disk electrode *vs* a Ag/AgCl reference electrode (black line) and at GLE *vs* a Ag/AgCl reference electrode (red line) or *vs* a gold pseudo-reference electrode (blue line) for a 1 mM hexacyanoferrate(II) solution in potassium nitrate 0.1 M. Scan rate 50 mVs^{-1}.

A potential shift towards the cathodic direction of 40 mV was found when the hexacyanoferrate(II) solution was analyzed at GLEs using the gold-pseudo reference electrode (Fig. 2, blue line).

Repeatable voltammograms were recorded, without observing any passivation of the electrode surface or any appreciable lowering of peak currents. Peak heights turned out to be repeatable for all concentrations with RSD ($n = 3$) of 2.0 %, as were also peak potentials (±5 mV).

Inter-electrode reproducibility was evaluated by testing seven different GLEs assembled by the method described above with the same 1 mM hexacyanoferrate(II) solution. These tests led to quite similar results in terms of peak current (±5.9 %), thus indicating that reproducible electrodes can be achieved by the procedure here proposed.

As it can be observed in Fig. 3 (left and inset), voltammograms recorded at scan rates from 5 to 200 mVs^{-1} led to a linear increase of the peak current with the square root of the scan rate. This linear dependence pointed out that the behavior of the tested GLEs complies with that expected for diffusion-controlled processes.

3.2. UV/Vis spectroelectrochemical characterization of GLEs

After performing these preliminary voltammetric tests, GLEs were placed inside the dedicated cell for spectroelectrochemical measurements. SEC measurements were performed in the normal mode, in which a reflection probe, consisting of 6 illumination optical fibres arranged around a central collection optical fibre, was placed slightly above the working electrode. Preliminary tests were carried out using a potassium hexacyanoferrate(II) solution at a concentration of 10 mM in 0.1 M of potassium nitrate by performing cyclic scans from −0.30 V to +0.60 V at a scan rate of 50 mVs^{-1}. This quasi-reversible system was used to optimize the operating conditions and to assess the influence of critical measurement parameters on the quality of the results.

With regard to its spectroscopic features, the 3d-t_{2g} orbital of ferrocyanide is filled with six electrons, whereas the 3d-t_{2g} orbital of ferricyanide has five electrons, which allows charge transfer from the ligand to the 3d-t_{2g} and from the t_{2g} to the e_g orbital, thus leading to two different spectra for these conjugated species in the UV/Vis region characterized by different absorption bands which are spectroscopically distinguishable [53]. In fact, ferricyanide exhibits two distinguishable absorption bands at 320 nm and 420 nm, while ferrocyanide does not exhibit any band in this region. The evolution of the band at 420 nm is usually used to monitor the conversion of ferrocyanide to ferricyanide [54].

As the oxidation of the ferrocyanide ion ($[Fe(CN)_6]^{4-}$) to ferricyanide progressed at the gold electrode surface during the anodic potential scan, the spectral evolution in the 350–800 nm region could be observed, as shown in Fig. 3 (right). At the beginning of the experiment (−0.10 V), when no oxidation process occurred, no absorption band was detected. As the applied potential at the electrode surface increased enough to allow the electrochemical oxidation process to start running, the appearance of the spectrum characteristic of ferricyanide was observed. The absorbance due to the formed ferricyanide ion increased progressively during the anodic scan and also continued in the initial part of the cathodic scan until the potential of +0.20 V was reached, at which the reduction to ferrocyanide began to take place. The spectra obtained suggested that the main difference is located in the region from 350 nm to 470 nm with an evident absorbing band centred at 420 nm.

Integration times between 10 and 100 ms were tested to establish the best optical sensitivity. An integration time of 15 ms enabled to achieve the best S/N ratio. In fact, lower times resulted in weaker spectra, while higher times led to stronger outputs but also to a loss of wavelength information due to the detector saturation.

The formation of the reaction product at the working electrode surface entailed the need to remove the GLE from the cell and to perform a series of washing operations after each scan. To evaluate the

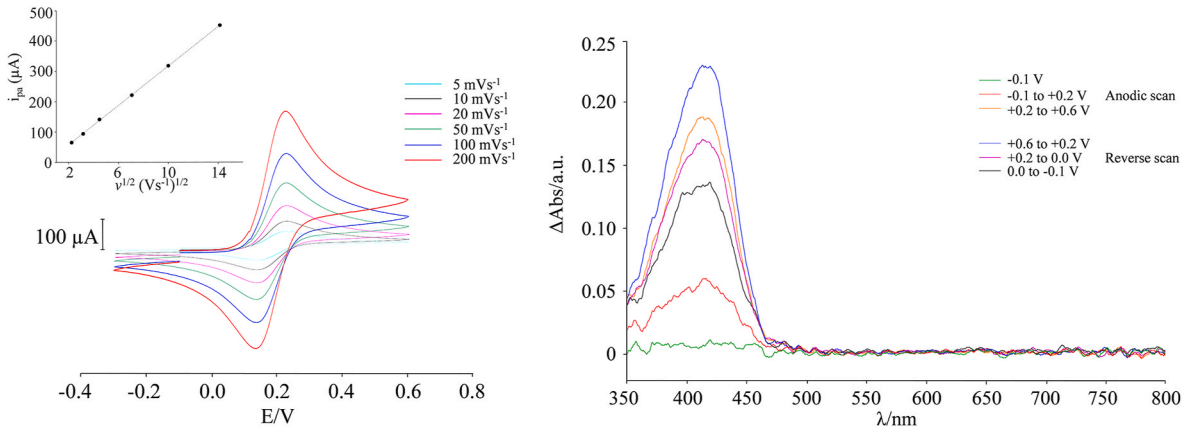

Fig. 3. Cyclic voltammograms recorded at a GLE *vs* a gold pseudo-reference electrode with the different reported scan rate for 10 mM potassium hexacyanoferrate(II) in 0.1 M KNO_3. Inset: correlation between anodic peak currents and square root of scan rate (left). Spectra evolution during the oxidation of 10 mM potassium hexacyanoferrate(II) in 0.1 M KNO_3. Scan rate 50 mVs^{-1}, $t_{integration}$ = 15 ms (right).

repeatability involved in these disassembly operations, a series of repeated tests were carried out using the same GLE and the same sample (potassium hexacyanoferrate(II)) at a concentration of 10 mM in 0.1 M potassium nitrate by measuring the corresponding peak currents and absorbance values. The results obtained showed that these operations led to satisfactory relative standard deviations (RSD ≤2.0 % and ≤2.8 % for EC and optical signals, respectively). Once again, no electrode passivation could be observed even when SEC tests were performed repeatedly.

When these tests were repeated using different GLEs, only a slightly higher standard deviations were found. RSD values ≤ 3.9 % and ≤5.5 % for electrochemical responses and optical signals, respectively, were in fact evaluated by detecting the response provided by five different GLEs prepared with the same procedure.

3.3. UV/Vis absorption spectroelectrochemistry of hydroxytyrosol

HTy was chosen as the model of ortho-diphenols in view of the fact that it is quantitatively and qualitatively the main phenolic antioxidant in olive oil, together with its precursors.

Aliquots (50 μL) of a 5 mM solution of this standard species dissolved in 20 mM H_2SO_4 were introduced in the spectroelectrochemical cell after the GLE was correctly located in the housing and the optical probe was positioned in a perpendicular position over the WE for SEC measurements. The choice of H_2SO_4 as the electrolyte was made in order to slow down as much as possible the kinetics of the chemical reaction between reducing species potentially present in olive oil and quinones generated during the electrochemical oxidation of ortho-diphenols [55, 56].

As expected, during cyclic voltammetric scans recorded at the scan rate of 50 mVs^{-1}, an anodic-cathodic system was observed consisting in an oxidation peak located at +0.35 V associated to a cathodic peak at about −0.20 V, as shown in Fig. 4 (left). In fact, it is well-known that in anodic scans ortho-diphenol moieties undergo a two-electron-two-proton oxidation process leading to their corresponding *o*-quinone form which are brought back into the catechol form in the reverse cathodic scan [57–59].

From the optical signals recorded simultaneously during SEC experiments (see Fig. 4, right), the appearance of an absorption band in the wavelength range from 280 to 480 nm, with a maximum absorption at about 395 nm, could be observed. This absorption band, typical of the generated quinone [60], grew as the faradic process at the gold electrode surface continued to occur, until it reached its maximum intensity in the backward scan when the potential approached +0.20 V, at which the reduction of the generated quinone started.

Also in this case, in order to remove the species produced by the electrochemical reaction from the solution and to eliminate any source of interference in the subsequent analyses, the cell had to be disassembled and washed thoroughly, together with the GLE itself.

Tests similar to those described above were performed using the same electrode and the same reference solution after reassembling the cell. It was thus possible to assess the good measurement repeatability, which were characterized by RSD of 1.3 % and 4.6 % for electrochemical and optical signals, respectively.

Once again, no passivation phenomenon was observed at the gold surface during these repeated measurements.

Also in this case, integration times between 10 and 100 ms were tested to individuate the best optical sensitivity, thus verifying that the

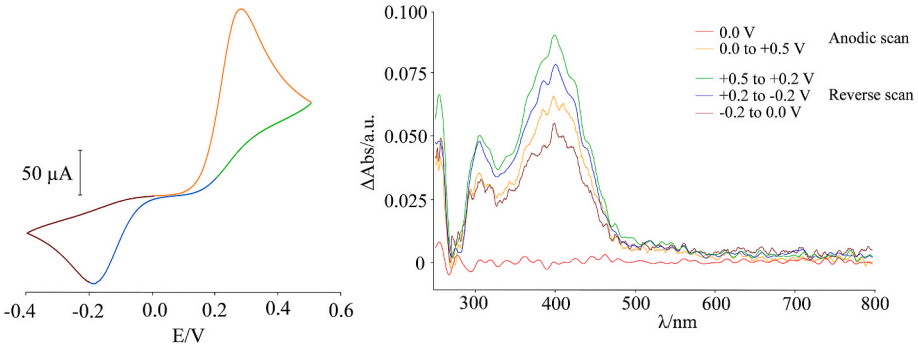

Fig. 4. Cyclic voltammograms recorded at a GLE *vs* a gold pseudo-reference electrode with a scan rate of 50 mVs^{-1} for 5 mM HTy in 20 mM H_2SO_4 (left). Spectra evolution during the oxidation of HTy. $t_{integration}$ = 15 ms (right).

most suitable integration time was 15 ms.

In order to assess the effect of possible interferences on the determination of HTy, further SEC investigations were carried out using a 5 mM solution of HTy to which 5 mM of Ty was added, i.e. a monophenolic species that, together with its precursors, is abundantly present in olive oil. As it can be seen from Fig. 5 and in agreement with previous investigations, the presence of Ty generated an anodic peak at +0.60 V, at more positive potentials than HTy, with no conjugated peak in the reverse scan.

Although in the first scan the presence of this compound did not affect neither the EC nor the optical signals, a decrease of the current intensity was progressively observed after repetitive scans performed by extending the potential at which the scan direction was reversed at values at which also Ty could be oxidized. This finding was conceivably ascribed to the progressive fouling of the gold surface, typically observed for the electrochemical oxidation of monophenols.

For this reason, all following tests aimed at determining HTy were carried out by narrowing the potential window up to +0.50 V, to avoid the oxidation of Ty possibly present in real samples.

Subsequently, the effect of the scan rate was evaluated to identify the best conditions to be used for the construction of the corresponding calibration plot and the subsequent quantification of HTy in real samples.

Also in this case, voltammograms recorded at scan rates from 5 to 200 mVs^{-1} led to a linear increase of the anodic peak current with the square root of the scan rate (see Fig. 6 left and inset). Once again, these linear dependences pointed out that the behavior of the tested GLEs comply with that expected for diffusion-controlled processes.

The intensity changes of the optical signal with the scan rate, calculated as the difference (ΔAbs) between the absorbance recorded during the scan, in the potential range where it reaches its maximum intensity, and that recorded at potential of 0 V, where no electrochemical process occurs, is reported in Fig. 6 (right).

As it can be seen from this recorded voltabsorptogram, which measures the absorbance signal at the wavelength of 395 nm during the voltammetric sweep, the scan rate used affected the optical response during the scan. A slow scan rate led to good optical signals but low currents, while high scan rates led to high current responses but low change in the absorbance with respect to the reference. Despite this change in intensity, the potential at which the maximum absorbance was recorded, corresponded to +0.20 V, where the reverse scan direction causes the quinone unit generated in the anodic scan to begin to be reduced.

On the basis of these SEC measurements, a scan rate of 10 mVs^{-1} was selected as the optimal for further analyses aimed at the construction of calibration plots. This value was inferred from the height of EC signals (Fig. 7, left), calculated at the anodic peak potential of +0.35 V and using the absorbance values (Fig. 7, right) recorded when the scan reached the potential of +0.20 V in the reverse can. As it can be observed, in both cases (see Fig. 7 insets) they showed a good linearity with the HTy concentrations in the range 50–10000 μM (equivalent to 7.71–1541.60 mg/L) and 200–10000 μM (equivalent to 30.83–1541.60 mg/L) for EC and optical detection, respectively.

The good detector sensitivities, together with the low noise level, resulted in low detection limits, evaluated for a S/N of 3, which turned out to be 18 μM and 73 μM (3.8 mg/L and 11.3 mg/mL) for EC and optical signals, respectively.

These detection limits make this approach suitable for the analysis of hydrophilic ortho-diphenols usually present in EVOOs (about 10–600 mg/kg) [12].

3.4. UV/Vis spectroelectrochemical determination of ortho-diphenols in extra virgin olive oil

GLEs were used to evaluate the ortho-diphenols content in different EVOO and sunflower oil samples exploiting the UV/Vis-SEC method described above. They were extracted by the procedure described in Section 2.4.

Voltammetric profiles recorded on EVOO real samples showed the anodic-cathodic system found in the analysis of the synthetic samples, with the sole difference that a very slight potential shift was observed.

This slight shift was conceivably due to the fact that the extraction process did not ensure complete removal of the lipid components from the analyzed samples, causing a slightly higher overpotential during detection. However, this contamination did not affect the repeatability of the measurements which were in any case carried out after disassembling and washing the cell and electrode as described for the tests conducted on synthetic samples.

Similarly, when the potential of +0.20 V in the reverse scan was reached, the optical response showed the appearance of the absorption band attributable to the corresponding quinone with the maximum absorbance at 395 nm.

The relevant peak heights and absorbance recorded during voltammetric and optical measurements were converted into ortho-diphenol concentrations by the calibration plots constructed for synthetic HTy samples.

Quantification of ortho-diphenols in oil samples, expressed as HTy equivalents, was attained with good sensitivity and repeatability. Concentrations of ortho-diphenols of 170.3 mg/kg (1105 μM) and 166.5 mg/kg (1080 μM) were detected in the two EVOOs samples analyzed by resorting to the combination of voltammetric and spectrophotometric measurements, with deviations which did not go beyond ±8.1 %.

The correctness of these findings was confirmed by measurements on EVOO samples after the addition of known amounts of HTy, to achieve additional concentrations of this phenolic compound equal of 400 or 800 μM. The increase of the height of the anodic peak and of the absorbance recorded after these additions were then compared with the calibration plots constructed for the pure analyte. The results obtained from these tests enabled to evaluate that under these conditions the recovery was equal to 87 ± 8 %. Very similar recovery values were

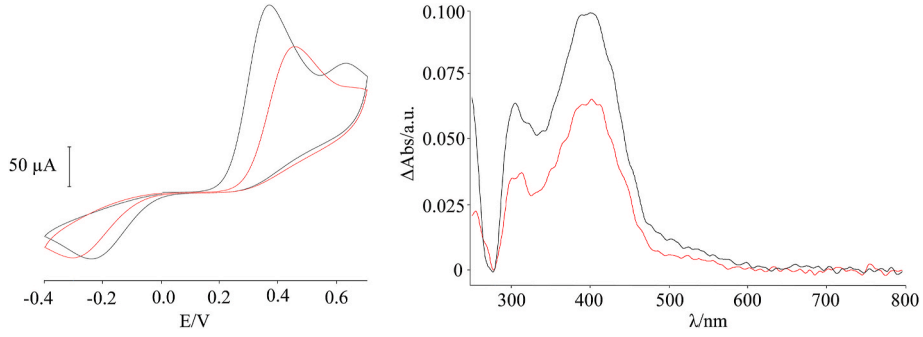

Fig. 5. First (black line) and second cyclic (red line) voltammograms recorded at a GLE *vs* a gold pseudo-reference electrode with a scan rate of 50 mVs^{-1} for a mixture of 5 mM HTy and 5 mM Ty in 20 mM H_2SO_4 (left). Spectra evolution during the oxidation of a mixture HTy and Ty. $t_{integration}$ = 15 ms (right).

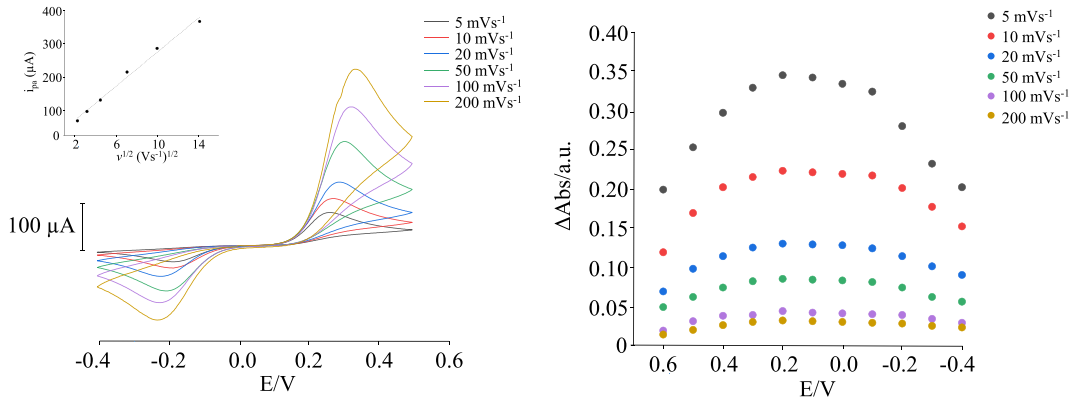

Fig. 6. Cyclic voltammograms recorded at a GLE *vs* a gold pseudo-reference electrode with a scan rate of 5, 10, 20, 50, 100, 200 mVs^{-1} for 5 mM of HTy in 20 mM H_2SO_4 (left) and correlation between current of anodic peaks and scan rate square root (inset). Voltabsorptogram recorded at 395 nm during the reverse scan at different scan rates (right).

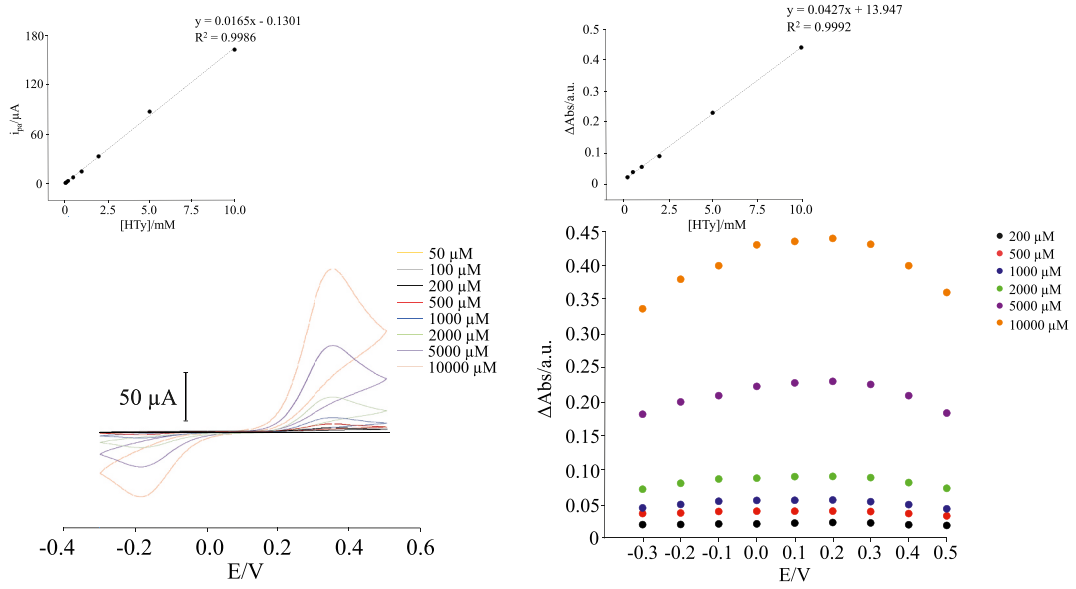

Fig. 7. Cyclic voltammograms (left) and voltabsorptogram recorded at 395 nm during the reverse scan (right) recorded at a GLE *vs* a gold pseudo-reference electrode for different concentrations of HTy in 20 mM H_2SO_4, together with calibration plots of the current peak at +0.35 V (inset, left) absorbance at 395 nm and at +0.20 V (inset, right) *vs* the HTy concentration.

obtained from the analysis of the sunflower oil sample fortified with a HTy concentration of 800 µM.

As it was emphasized previously, HTy in olive oil is also present in more complex structures such as oleuropein and other glycosides, and hydrolysis in an acidic environment was required for its release from these species. The method developed based on the oxidation of the catechol moiety present in all HTy derivatives allowed their direct quantification without the need for further steps after extraction to break the glycone-aglycone bond. The ortho-diphenol contents thus determined were in fairly good agreement (±14 %) with those found by us analyzing the same samples with the sodium molybdate colorimetric approach [61,62].

As to the analysis of the sunflower oil sample, no trace of hydrophilic ortho-diphenols was instead detected. This finding points out that the method here proposed can be profitably adopted for the rapid discrimination of edible oils.

In order to make a comparison with the electrochemical methods reported in the literature for the determination of ortho-diphenol compounds in olive oil samples, peculiarities of each approach are reported in Table 1. As it can be seen, in some cases, more complex sample preparation procedures are employed that require higher consumption of organic solvents. Furthermore, some methods use electrochemical devices characterized by quite complex electrode surface modifications.

4. Conclusions

In this paper, an innovative approach for the construction of electrode cells with a planar configuration using gold leaf as electrode material is presented. These electrodes can be a valid alternative to disk electrodes and screen-printed electrodes and can be easily assembled even in situations where access to complex instrumentation is limited. Furthermore, they are characterized by low cost and quick replicability.

Compared with the manufacturing methods proposed in the literature, the approach proposed here for the fabrication of gold leaf electrodes does not require the use of either glues or solvents [26]. It can also be handled by non-expert personnel as it does not require complex instrumentation such as laser ablation systems or similar technologies [24]. Furthermore, unlike other methods involving the fabrication of the sole working electrode [23,25], while reference and counter electrodes are assembled separately using different materials, this method enables the simultaneous and highly repeatable fabrication of all the three electrodes of electrochemical cells.

Table 1
Comparative features of previously reported electrochemical methods for ortho-diphenols determination in olive oil samples.

Device/Electrode	EC technique	Sample preparation	LOD	Ref.
Paper-strip with IR laser nanodecorated graphene ink-based working electrode	Differential pulse voltammetry	EVOO samples (4 μL) were loaded onto the drop spot and then introduced in the fluidic channel using DMSO (5 μL). Phosphate buffer (40 μL) was pipetted to carry analytes to the detection zone.	$LOD_{HTy} = 2$ μM; $LOD_{Oleu} = 0.6$ μM	[63]
Paper-based platform with an integrated pencil-drawn dual amperometric detector	Amperometric flow injection	Oil samples (2g) were extracted by vortex mixing and centrifugation with an 80/20 % v/v acetonitrile-water solution (2 mL). The procedure was repeated twice and the two extracted phases were mixed together and washed with pentane (4 mL) and then reconstituted to 4 mL with water.	$LOD_{HTy} = 8$ μM	[55]
Mo-MW-CNT-NH_2 modified screen printed electrode	Amperometric flow injection	Not declared	Not declared	[64]
Screen-printed carbon electrodes	Differential pulse voltammetry	1 or 0.150 g (depending on the oil) of sample were diluted to 5 mL with hexane. Then, 100 μL of aqueous 1 M HCl solution were added and the mixture was shaken for 2 min using vortex agitation The phases were separated by centrifugation and the remaining acidic aqueous phase was retrieved with a syringe for final analysis.	LOD = 0.022 mg/L reported for caffeic acid	[65]
Carbon based screen-printed electrode modified with carbon nanotubes and tyrosinase	Cyclic voltammetry	EVOO samples (5 g) were mixed with a 4:1 methanol-water solution. After centrifugation the supernatant was recovered and added to a phosphate buffer solution for analysis.	$LOD_{HTy} = 34.9$ nM	[66]
Screen printed carbon electrodes	Square wave voltammetry	Oil samples (25 g) was dissolved in hexane (25 mL) and polar compounds was extracted with a mixture of methanol-water (3:2, v/v, 3 × 15 mL).	$LOD_{HTy} = 0.40$ μM	[67]
Pencil-drawn paper based electrochemical detector at the end of a cotton thread fluidic channel in wall-jet configuration.	Amperometric flow injection	Same as ref [55]	$LOD_{HTy} = 2$ μM	[50]
Carbon black (CB) and molybdenum disulfide (MoS2) modified screen printed electrodes	Differential pulse voltammetry	EVOO 1 g was dissolved in 5 mL of hexane, and the solution was loaded onto an octadecyl C18 cartridges (1 g, 6 mL) The column was first eluted with 2 × 5 mL of hexane and then with 2 × 10 mL of methanol. The elute was placed in a conical flask and evaporated to dryness at room temperature (30 °C, 150 RPM) in a rotary evaporator. The extract was recovered with 0.5 mL of methanol.	$LOD_{Oleu} = 0.1$ μM; $LOD_{HTy} = 1$ μM	[68]
Planar electrochemical cells based on gold-leaf electrodes	Spectroelectrochemistry	Hydrophilic phenols were extracted by vortex mixing (1 min) 2 g of oil sample with 2 mL of a methanol-water solution (80/20 % v/v). The mixture was centrifuged (5000 rpm for 25 min) and the surnatant transferred into a 10 mL flask. The polar phase was washed with 2 mL of pentane and the solution was concentrated to 300 μL by air flowing. It was finally reconstituted with 300 μL of 20 mM H_2SO_4 aqueous solution before analysis.	$LOD_{HTy} = 18$ μM for EC and 73 μM for optical signals.	This work

Exploiting the typical characteristics of gold, which, like other metals, is characterized by high reflectivity, these GLEs based cells were used for the first time to perform spectroelectrochemical measurements in the reflectance mode. This technique makes it possible to combine the advantages of both optical and electrochemical detection modes and, even if it is used mainly to obtain useful information on mechanistic aspects, it has great and still partially unexplored potentiality to carry out quantitative determinations.

In fact, as demonstrated for the first time in this work, this analytical approach was adopted for the determination of ortho-diphenol antioxidants presents in EVOOs by exploiting the electrochemical oxidation of the catechol group to *o*-quinone, followed by its optical detection.

These combined chemical informations (electrochemical and spectroscopic) make it possible to obtain self-validated results in a short analysis time and using low sample volumes. This proposed optical-electrochemical combination can be profitably used to conduct rapid tests for easily distinguishing extra virgin olive oils from other vegetable oils, as well as to estimate their shelf life and their state of preservation.

CRediT authorship contribution statement

Michele Abate: Investigation, Formal analysis, Data curation, Conceptualization. **Gino Bontempelli:** Writing – review & editing. **Nicolò Dossi:** Writing – review & editing, Supervision, Resources, Methodology, Conceptualization.

Declaration of competing interest

The authors declare that they have no known competing financial interests or personal relationships that could have appeared to influence the work reported in this paper.

Data availability

No data was used for the research described in the article.

References

[1] A. Gałuszka, Z. Migaszewski, J. Namieśnik, The 12 principles of green analytical chemistry and the significance mnemonic of green analytical practices, Trac. Trends Anal. Chem. 50 (2013) 78–84, https://doi.org/10.1016/j.trac.2013.04.010.
[2] E. Psillakis, F. Pena-Pereira, The twelve goals of circular analytical chemistry, Trac. Trends Anal. Chem. 175 (2024) 117686, https://doi.org/10.1016/j.trac.2024.117686.
[3] F. Chemat, S. Garrigues, M. de la Guardia, Portability in analytical chemistry: a green and democratic way for sustainability, Curr. Opin. Green Sustainable Chem. 19 (2019) 94–98, https://doi.org/10.1016/j.cogsc.2019.07.007.
[4] M. Pontie, S.F. Mbokou, J. Dron, M.L. Chelaghmia, L. Schwartz, P. Asfar, Development of unmodified and CTAB-modified carbon paste electrodes (CPE) for direct electrochemical analysis of nitrites in aquarium water and rat blood, J. Appl. Electrochem. 53 (2023) 1701–1713, https://doi.org/10.1007/s10800-023-01872-5.
[5] M. Mallesha, R. Manjunatha, G.S. Suresh, J.S. Melo, S.F. D'Souza, T.V. Venkatesha, Direct electrochemical non-enzymatic assay of glucose using functionalized graphene, J. Solid State Electrochem. 16 (2012) 2675–2681, https://doi.org/10.1007/s10008-012-1674-y.

[6] A. García-Miranda Ferrari, S.J. Rowley-Neale, C.E. Banks, Screen-printed electrodes: transitioning the laboratory in-to-the field, Talanta Open 3 (2021) 100032, https://doi.org/10.1016/j.talo.2021.100032.

[7] S.R. Benjamin, F. de Lima, V.A. do Nascimento, G.M. de Andrade, R.B. Oriá, Advancement in paper-based electrochemical biosensing and emerging diagnostic methods, Biosensors 13 (2023) 689, https://doi.org/10.3390/bios13070689.

[8] G.P. Siqueira, D.A.G. Araújo, L.V. de Faria, D.L.O. Ramos, T.A. Matias, E. M. Richter, T.R.L.C. Paixão, R.A.A. Muñoz, A novel 3D-printed graphite/polylactic acid sensor for the electrochemical determination of 2,4,6-trinitrotoluene residues in environmental waters, Chemosphere 340 (2023) 139796, https://doi.org/10.1016/j.chemosphere.2023.139796.

[9] K.C. Honeychurch, The voltammetric behaviour of lead at a hand drawn pencil electrode and its trace determination in water by stripping voltammetry, Anal. Methods 7 (2015) 2437, https://doi.org/10.1039/c4ay02987a.

[10] I.A. de Araujo Andreotti, L.O. Orzari, J.R. Camargo, R.C. Faria, L.H. Marcolino-Junior, M.F. Bergamini, A. Gatti, B.C. Janegitz, Disposable and flexible electrochemical sensor made by recyclable material and low cost conductive ink, J. Electroanal. Chem. 840 (2019) 109–116, https://doi.org/10.1016/j.jelechem.2019.03.059.

[11] F.C. Vicentini, T.A. Silva, O. Fatibello-Filho, Carbon black electrodes applied in electroanalysis, Curr. Opin. Electrochem. 43 (2024) 101415, https://doi.org/10.1016/j.coelec.2023.101415.

[12] N. Dossi, R. Toniolo, F. Impellizzieri, G. Bontempelli, Doped pencil leads for drawing modified electrodes on paper-based electrochemical devices, J. Electroanal. Chem. 722–723 (2014) 90–94, https://doi.org/10.1016/j.jelechem.2014.03.038.

[13] M. Zamani, V. Yang, L. Maziashvili, C.M. Klapperich, A.L. Furst, Surface requirements for optimal biosensing with disposable gold electrodes, ACS Meas. Sci. Au 2 (2022) 91–95, https://doi.org/10.1021/acsmeasuresciau.1c00042.

[14] M. Zamani, C.M. Klapperich, A.L. Furst, Recent advances in gold electrode fabrication for low-resource setting biosensing, Lab Chip 23 (2022) 1410, https://doi.org/10.1039/d2lc00552b.

[15] M.F. Md Noh, I.E. Tothill, Development and characterisation of disposable gold electrodes, and their use for lead(II) analysis, Anal. Bioanal. Chem. 386 (2006) 2095–2106, https://doi.org/10.1007/s00216-006-0904-5.

[16] Y. Li, P.C.H. Li, M. Parameswaran, H.-Z. Yu, Inkjet printed electrode arrays for potential modulation of DNA self-assembled monolayers on gold, Anal. Chem. 80 (2008) 8814–8821, https://doi.org/10.1007/s00216-006-0904-5.

[17] Y. Sui, Y. Dai, C.C. Liu, R.M. Sankaran, C.A. Zorman, A new class of low-temperature plasma-activated, inorganic salt-based particle-free inks for inkjet printing metals, Adv. Mater. Technol. 4 (2019) 1900119, https://doi.org/10.1002/admt.201900119.

[18] C. Hu, X. Bai, Y. Wang, W. Jin, X. Zhang, S. Hu, Inkjet printing of nanoporous gold electrode arrays on cellulose membranes for high-sensitive paper-like electrochemical oxygen sensors using ionic liquid electrolytes, Anal. Chem. 84 (2012) 3745–3750, https://doi.org/10.1021/ac3003243.

[19] G.C. Jensen, C.E. Krause, G.A. Sotzing, J.F. Rusling, Inkjet-printed gold nanoparticle electrochemical arrays on plastic. Application to immunodetection of a cancer biomarker protein, Phys. Chem. Chem. Phys. 13 (2011) 4888–4894, https://doi.org/10.1039/c0cp01755h.

[20] J.R. Camargo, L.O. Orzari, P.R. de Oliveira, D.A. Gouveia Araújo, C. Kalinke, D. P. Rocha, A.L. dos Santos, R.M. Takeuchi, R.A. Abarza Munoz, J.A. Bonacin, B. Campos Janegitz, Development of conductive inks for electrochemical sensors and biosensors, Microchem. J. 164 (2021) 105998, https://doi.org/10.1016/j.microc.2021.105998.

[21] M.S.F. Santos, W.A. Ameku, I.G.R. Gutz, T. R. L. C. Gold leaf, From gilding to the fabrication of disposable, wearable and lowcost electrodes, Talanta 179 (2018) 507–511, https://doi.org/10.1016/j.talanta.2017.11.021.

[22] M. Zamani, J.M. Robson, A. Fan, M.S. Bono, A.L. Furst, C.M. Klapperich, Electrochemical strategy for low-cost viral detection, ACS Cent. Sci. 7 (2021) 963–972, https://doi.org/10.1021/acscentsci.1c00186.

[23] K.H. Alqibthiyah, P. Prasertying, T. Techarang, W. Kamsong, H. Sulistyarti, K. Uraisin, D. Nacapricha, Gold leaf electrochemical flow cell for determination of iodide in nuclear emergency tablets, Talanta 275 (2024) 125963, https://doi.org/10.1016/j.talanta.2024.125963.

[24] I. Podunavac, M. Kukkar, V. Léguillier, F. Rizzotto, Z. Pavlovic, L. Janjušević, V. Costache, V. Radonic, J. Vidic, Low-cost gold leaf electrode as a platform for Escherichia coli immunodetection, Talanta 259 (2023) 124557, https://doi.org/10.1016/j.talanta.2023.124557.

[25] P. Prasertying, N. Jantawong, T. Sonsa-ard, T. Wongpakdee, N. Khoonrueng, S. Bukingd, D. Nacapricha, Gold leaf electrochemical sensors: applications and nanostructure modification, Analyst 146 (2021) 1579–1589, https://doi.org/10.1039/D0AN02455D.

[26] J.R. Camargo, S. Cleto, A. Neumann, D.C. Azzi, R.D. Crapnell, C.E. Banks, B. C. Janegitz, Edible gold leaf as a viable modification method for screen-printed sensors, Electrochim. Acta 478 (2024) 143825, https://doi.org/10.1016/j.electacta.2024.143825.

[27] C. Grazioli, E. Lanza, M. Abate, G. Bontempelli, N. Dossi, Lab-on kit: a 3D printed portable device for optical and electrochemical dual-mode detection, Talanta 275 (2024) 126185, https://doi.org/10.1016/j.talanta.2024.126185.

[28] M.H.M. Facure, R.S. Andre, R.M. Cardoso, L.A. Mercante, D.S. Correa, Electrochemical and optical dual-mode detection of phenolic compounds using MnO_2/GQD nanozyme, Electrochim. Acta 441 (2023) 141777, https://doi.org/10.1016/j.electacta.2022.141777.

[29] K. Lal, S.A. Jaywant, K.M. Arif, Electrochemical and optical sensors for real-time detection of nitrate in water, Sensors 23 (2023) 7099, https://doi.org/10.3390/s23167099.

[30] F. Sekli Belaïdi, L. Farouil, L. Salvagnac, P. Temple-Boyera, I. Séguya, J.L. Heully, F. Alary, E. Bedel-Pereira, J. Launay, Towards integrated multi-sensor platform using dual electrochemical and optical detection for on-site pollutant detection in water, Biosens. Bioelectron. 132 (2019) 90–96, https://doi.org/10.1016/j.bios.2019.01.065.

[31] T. Salzillo, A. Marchetti, J. Vejpravova, P. Fanjul Bolado, C. Fontanesi, Molecular electrochemistry. An overview of a crossfield: electrochemistry/spectroscopic/theoretical integrated approach, Curr. Opin. Electrochem. 35 (2022) 101072, https://doi.org/10.1016/j.coelec.2022.101072.

[32] J. Garoz-Ruiz, J.V. Perales-Rondon, A. Heras, A. Colina, Spectroelectrochemical sensing: current trends and challenges, Electroanalysis 31 (2019) 1254–1278, https://doi.org/10.1002/elan.201900075.

[33] J.J.A. Lozeman, P. Führer, W. Olthuis, M. Odijk, Spectroelectrochemistry, the future of visualizing electrode processes by hyphenating electrochemistry with spectroscopic techniques, Analyst 145 (2020) 2482–2509, https://doi.org/10.1039/c9an02105a.

[34] L. León, J.D. Mozo, Designing spectroelectrochemical cells: a review, Trac. Trends Anal. Chem. 102 (2018) 147–169, https://doi.org/10.1016/j.trac.2018.02.002.

[35] F. Olmo-Alonso, J. Garoz-Ruiz, A. Heras, A. Colina, Normal or parallel configuration in spectroelectrochemistry? Bidimensional spectroelectroanalysis in presence of an antioxidant compound, J. Electroanal. Chem. 935 (2023) 177993, https://doi.org/10.1016/j.jelechem.2023.117333.

[36] Y. Shi, S. Ward, C. Riley, D.J. Sirbuly, Multifunctional microcoaxial fibres for electrochemical, optical and spectroelectrochemical sensing, Sens. Actuator B-Chem. 394 (2023) 134361, https://doi.org/10.1016/j.snb.2023.134361.

[37] M. Perez-Estebanez, J.V. Perales-Rondon, S. Hernandez, A. Heras, A. Colina, Bidimensional spectroelectrochemistry with tunable thin-layer thickness, Anal. Chem. 96 (2024) 9927–9934, https://doi.org/10.1021/acs.analchem.4c01132.

[38] S.H. Kim, J.W. Lee, I.-H. Yeo, Spectroelectrochemical and electrochemical behavior of epinephrine at a gold electrode, Electrochim. Acta 45 (2000) 2889–2895, https://doi.org/10.1016/S0013-4686(00)00364-9.

[39] I.S. Zavarine, C.P. Kubiak, A versatile variable temperature thin layer reflectance spectroelectrochemical cell, J. Electroanal. Chem. 495 (2001) 106–109, https://doi.org/10.1016/S0022-0728(00)00394-6.

[40] D. Ibáñez, M.B. González-García, D. Hernández-Santos, P. Fanjul-Bolado, Detection of dithiocarbamate, chloronicotinyl and organophosphate pesticides by electrochemical activation of SERS features of screen-printed electrodes, Spectroc. Acta Pt. A-Molec. Biomolec. Spectr. 248 (2021), https://doi.org/10.1016/j.saa.2020.119174.

[41] F. Olmo, A. Rodriguez, A. Colina, A. Heras, UV/Vis absorption spectroelectrochemistry of folic acid, J. Solid State Electrochem. 102 (2022) 147–169, https://doi.org/10.1007/s10008-021-05026-5.

[42] N. González-Diéguez, A. Colina, J. López-Palacios, A. Heras, Spectroelectrochemistry at screen-printed electrodes: determination of dopamine, Anal. Chem. 84 (2012) 9146–9153, https://doi.org/10.1021/ac3018444.

[43] D. Ibáñez, M.B. González-García, D. Hernández-Santos, P. Fanjul-Bolado, Spectroelectrochemical enzyme sensor system for acetaldehyde detection in wine, Biosensors 12 (2022) 1032, https://doi.org/10.3390/bios12111032.

[44] M. El Boutaybi, A. Titi, A.Y.A. Alzahrani, Z. Bahari, M. Tillard, B. Hammouti, R. Touzani, Aerial oxidation of phenol/catechol in the presence of catalytic amounts of [(Cl)2Mn(RCOOET)], RCOOET=Ethyl-5-Methyl-1-(((6-Methyl-3-Nitropyridin-2-yl)Amino)Methyl)-1H-Pyrazole-3-Carboxylate, Catalysts 12 (2022) 1642, https://doi.org/10.3390/catal12121642.

[45] M. De Lucia, L. Panzella, A. Pezzella, A. Napolitano, M. d'Ischia, Oxidative chemistry of the natural antioxidant hydroxytyrosol: hydrogen peroxide-dependent hydroxylation and hydroxyquinone/o-quinone coupling pathways, Tetrahedron 62 (2006) 1273–1278, https://doi.org/10.1016/j.tet.2005.10.055.

[46] K.L. Tuck, P.J. Hayball, I. Stupans, Structural characterization of the metabolites of hydroxytyrosol, the principal phenolic component in olive oil, in rats, J. Agric. Food Chem. 50 (2020) 2404–2409, https://doi.org/10.1021/jf011264n.

[47] M. Bertelli, A.K. Kiani, S. Paolacci, E. Manara, D. Kurti, K. Dhuli, V. Bushati, J. Miertus, D. Pangallo, M. Baglivo, T. Beccari, S. Michelini, Hydroxytyrosol: a natural compound with promising pharmacological activities, J. Biotechnol. 309 (2020) 29–33, https://doi.org/10.1016/j.jbiotec.2019.12.016.

[48] E.F. Newair, M. Khairy, M. Ismael, A. Al-Anazi, R.J. White, D.D. Dionysiou, Monitoring the oxidative function of hydroxytyrosol and potential interactions with glutathione produced by human cells, Microchem. J. 197 (2024) 109863, https://doi.org/10.1016/j.microc.2023.109863.

[49] F. Velotti, R. Bernini, Hydroxytyrosol Interference with inflammaging via modulation of inflammation and autophagy, Nutrients 15 (2023) 1774, https://doi.org/10.3390/nu15071774.

[50] N. Dossi, R. Toniolo, F. Terzi, N. Sdrigotti, F. Tubaro, G. Bontempelli, A cotton thread fluidic device with a wall-jet pencil-drawn paper based dual electrode detector, Anal. Chim. Acta 1040 (2018) 74–80, https://doi.org/10.1016/j.aca.2018.06.061.

[51] N. Nenadis, A. Mastralexi, M.Z. Tsimidou, S. Vichi, B. Quintanilla-Casas, J. Donarski, V. Bailey-Horne, B. Butinar, M. Miklavčič, D.L. García González, T. Gallina Toschi, Toward a harmonized and standardized protocol for the determination of total hydroxytyrosol and tyrosol content in virgin olive oil (VOO). Extraction solvent, Eur. J. Lipid Sci. Technol. 120 (2018) 1800099, https://doi.org/10.1002/ejlt.201800099.

[52] International Olive Council (IOC), Determination of Biophenols in Olive Oil by HPLC; COI/T.20/Doc, 2009. No. 29IOC: Madrid, Spain.

[53] S. Kishioka, Higher-order derivative electronic absorption spectroscopy of ferricyanide electrogenerated in situ by optically transparent thin layer electrochemical cell, J. Electroanal. Chem. 918 (2022) 116485, https://doi.org/10.1016/j.jelechem.2022.116485.
[54] L. León, J.J. Maraver, J. Carbajo, J.D. Mozo, Simple and multi-configurational flow-cell detector for UV-vis spectroelectrochemical measurements in commercial instruments, Sens. Actuator B-Chem. 186 (2013) 263–293, https://doi.org/10.1016/j.snb.2013.06.024.
[55] N. Dossi, R. Toniolo, F. Impellizzieri, F. Tubaro, G. Bontempelli, F. Terzi, E. Piccin, A paper-based platform with a pencil-drawn dual amperometric detector for the rapid quantification of ortho-diphenols in extravirgin olive oil, Anal. Chim. Acta 950 (2017) 41–48, https://doi.org/10.1016/j.aca.2016.11.030.
[56] N.S. Isaacs, R. van Eldik, A mechanistic study of the reduction of quinones by ascorbic acid, J. Chem. Soc.-Perkin Trans. 2 (1997) 1465–1468, https://doi.org/10.1039/A701072I.
[57] M.L. de Malezieu, S. Ferron, A. Sauvager, P. Courtel, C. Ramassamy, S. Tomasi, M.-L. Abasq, UV-Vis spectroelectrochemistry of oleuropein, tyrosol, and p-coumaric acid individually and in an equimolar combination. differences in LC-ESI-MS2 profiles of oxidation products and their neuroprotective properties, Biomolecules 9 (2019) 802, https://doi.org/10.3390/biom9120802.
[58] T.A. Enache, A. Amine, C.M.A. Brett, A.M. Oliveira-Brett, Virgin olive oil ortho-phenols-electroanalytical quantification, Talanta 105 (2013) 179–186, https://doi.org/10.1016/j.talanta.2012.11.055.
[59] N. Dossi, R. Toniolo, F. Terzi, E. Piccin, G. Bontempelli, Simple pencil-drawn paper-based devices for one-spot electrochemical detection of electroactive species in oil samples, Electrophoresis 36 (2015) 1830–1836, https://doi.org/10.1002/elps.201500083.
[60] I. Di Maio, S. Esposto, A. Taticchi, R. Selvaggini, G. Veneziani, S. Urbani, M. Servili, HPLC-ESI-MS investigation of tyrosol and hydroxytyrosol oxidation products in virgin olive oil, Food Chem. 125 (2011) 21–28, https://doi.org/10.1016/j.foodchem.2010.08.025.
[61] S. Gómez-Alonso, M.D. Salvador, G. Fregapane, Phenolic compounds profile of cornicabra virgin olive oil, J. Agric. Food Chem. 50 (2002) 6812–6817, https://doi.org/10.1021/jf0205211.
[62] T. Gutfinger, Polyphenols in olive oils, J. Am. Oil Chem. Soc. 58 (1981) 966–968, https://doi.org/10.1007/BF02659771.
[63] F. Silveri, A. Scroccarello, F. Della Pelle, M. Del Carlo, D. Compagnone, Rapid pretreatment-free evaluation of antioxidant capacity in extra virgin olive oil using a laser-nanodecorated electrochemical lab-on-strip, Food Chem. 420 (2023) 136112, https://doi.org/10.1016/j.foodchem.2023.136112.
[64] M. Del Carlo, A. Amine, M. Haddam, F. della Pelle, G.C. Fusella, D. Compagnone, Selective voltammetric analysis of o-diphenols from olive oil using Na_2MoO_4 as electrochemical mediator, Electroanalysis 24 (2012) 889–896, https://doi.org/10.1002/elan.201100603.
[65] E. Fernández, L. Vidal, A. Canals, Rapid determination of hydrophilic phenols in olive oil by vortex-assisted reversed-phase dispersive liquid-liquid microextraction and screen-printed carbon electrodes, Talanta (2018) 44–51, https://doi.org/10.1016/j.talanta.2017.12.075.
[66] A.V. Bounegru, C. Apetrei, Sensitive detection of hydroxytyrosol in extra virgin olive oils with a novel biosensor based on single-walled carbon nanotubes and tyrosinase, Int. J. Mol. Sci. 23 (2022) 9132, https://doi.org/10.3390/ijms23169132.
[67] T.A. Enache, A. Amine, C.M.A. Brett, A.M. Oliveira-Brett, Virgin olive oil ortho-phenols electroanalytical quantification, Talanta 105 (2013) 179–186, https://doi.org/10.1016/j.talanta.2012.11.055.
[68] D. Rojas, F. Della Pelle, M. Del Carlo, E. Fratini, A. Escarpa, D. Compagnone, Nanohybrid carbon black-molybdenum disulfide transducers for preconcentration-free voltammetric detection of the olive oil o-diphenols hydroxytyrosol and oleuropein, Microchim. Acta 186 (2019) 363, https://doi.org/10.1007/s00604-019-3418-5.